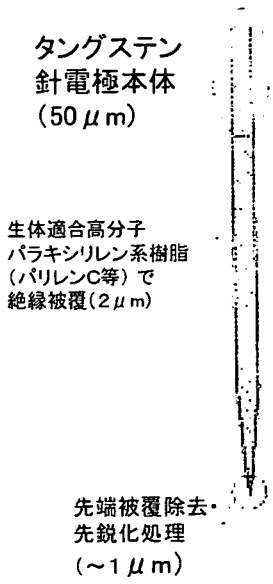

先ず実際に動物神経でテストするためのW鍼用の台座構造案を考えた。下図に示すように、一対をなすW鍼の間隔を100～500μmとし、図のような穴間隔の異なる複数(10本)の鍼を1つの樹脂台座にAu線を絡めた上体で植え込み、Si接着剤などで固定する構造を考えた。この電極アレイを、ウサギ腓骨・脛骨神経への刺入するテストによって、神経膜貫通性や強度の点から針シャフト径を50μmと決定した。また、神経束内に交感神経線維が大半を占めると考えられる腎臓交感神経に電極アレイを装着した所、腎臓交感神経活動を記録できた。そこで、装置の２次試作へと開発を進めた。

３．W針電極アレイの２次試作

２次試作装置の基本構成と製作プロセス概略を示す。

プロセス１

Ｓｉフィードスルー電極付マイコンデバイスチップ

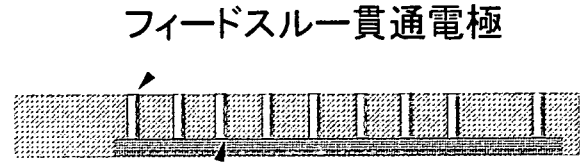

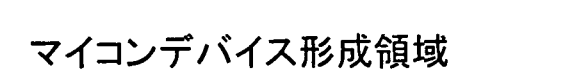

プロセス２

Ｓｉフィードスルー Ｃｕ埋め込み

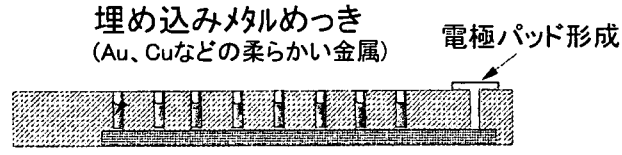

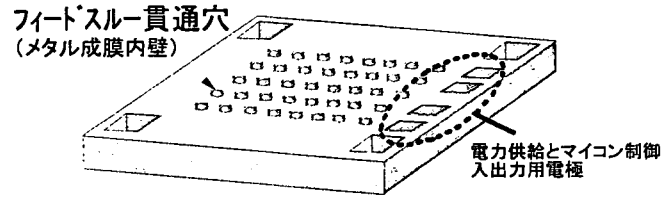

プロセス３

鍼付ベースとマイコンチップの合体

(鍼電極とマイコンの接続)

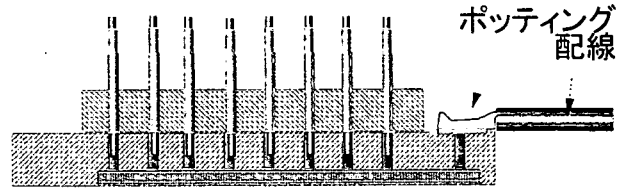

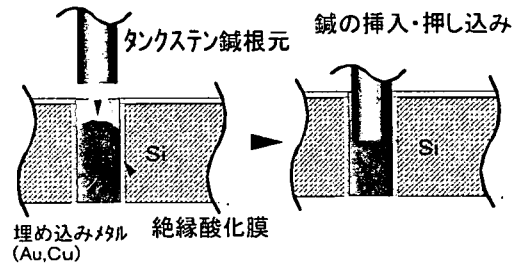

実際に、W針を電極間隔100μmに2列12ピン集積化した装置を下に示す。これは、世界最小レベルの電極アレイの神経装置である。ヒト自律神経モニターに用いる神経は直径0.5－1.5 cmであり、この仕様で50―150本の針電極を１本の神経に挿入できるため、この電極アレイは、実用に十分な空間分解能（神経線維選択能）であると考えられる。

＜装置全体＞

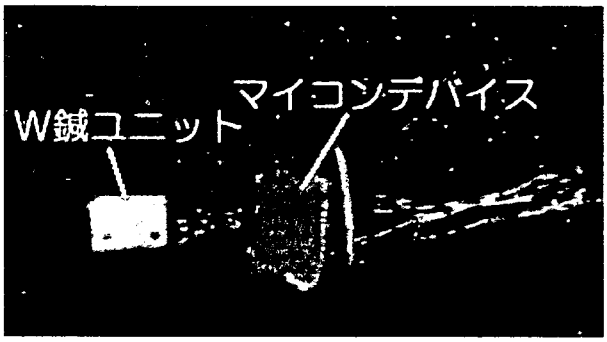

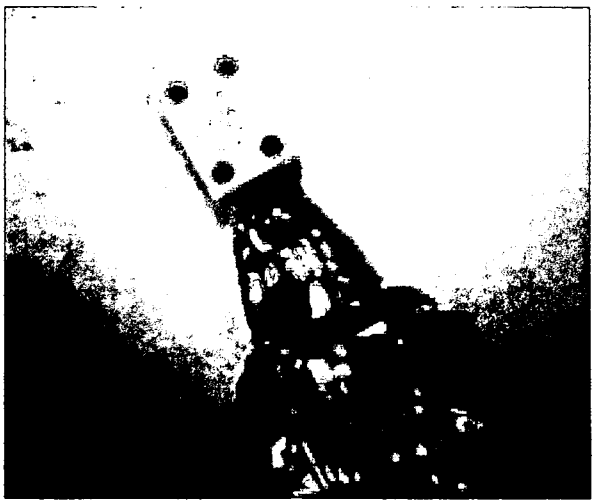

＜電極アレイ＞

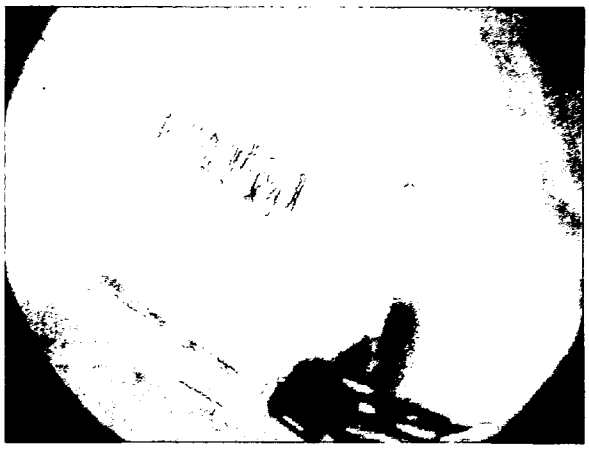

４．意識化動物のおける慢性使用へ向けた神経装置の改良

４－１．鍼デバイスの改良

長期間使用に耐えるようＭＥＭＳ加工によって神経装置を改良した。針デバイス部はまず、Si製装置台座の裏面に針電極受部を形成（ウェットエッチング）、台座表面から針穴を貫通（ドライエッチング）、Si全面を絶縁被膜（熱酸化法）、酸化膜上にAu/Pt/Tiスパッタ成膜、フォトリソで配線パターン形成したフィードスルー基板を製作した。次に、裏面側から針電極を挿入、導電性樹脂でAu配線と導通、硬化型樹脂で電極固定、配線引き出しパッドからAu細線を接続、底板とSi台座をSi接着剤で接着し、裏面配線・電極部を完全シール保護した。この工程により電極・配線の接続・固定を格段に強固にできた。

４－１－１．プロセスフロー

Wの鍼を立てて固定し、配線を取り出すベース部分をSiウエハを使ったリソグラフ技術とエッチング及び成膜技術により作成した。下にプロセスフローを示す。

Si製鍼ベース部材製作プロセス

	大 工 程	断面図	プロセス	使用装置
1	Siウエハ熱酸化	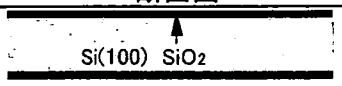	(100)高抵抗(1kΩcm) 3インチ, 0.2mmt スチーム酸化(1100℃)	酸化炉
2	リソグラフ(段差形成)		酸化膜ﾊﾟﾀｰﾆﾝｸﾞ BHF処理	ウエットエッチング器具
3	異方性ウエットエッチング		THAH処理 (アルカリエッチング)	アルカリエッチング処理装置
4	リソグラフ(貫通孔形成)		裏面酸化膜ﾊﾟﾀｰﾆﾝｸﾞ BHF処理	ウエットエッチング器具
5	異方性ドライエッチング	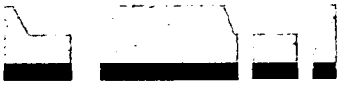	DRIE処理 (Deep reactive Ion Etching)	DRIE装置
6	再熱酸化		スチーム酸化 (1100℃) 1.5μm	酸化炉
7	メタルスパッタ		Au/Pt/Ti (300/250/500nm)	3元スパッタ装置
8	リソグラフ(メタライズ)	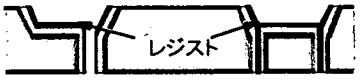	ミリング(Arドライエッチング	ミリング装置
9	洗浄・小片化		カッティング	ダイシング装置

チップ寸法

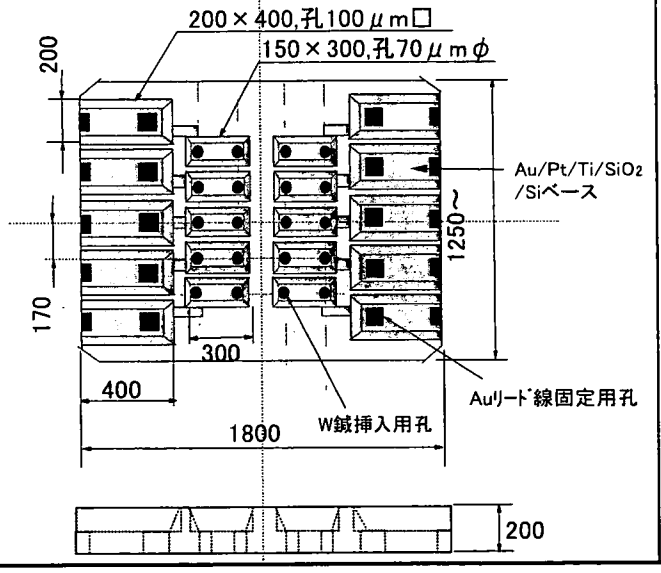

チップ実物写真（表・裏）

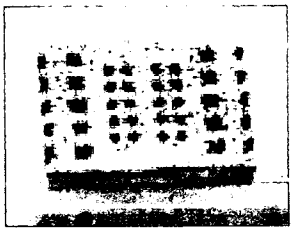

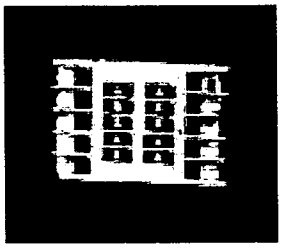

4－1－2．W鍼の製作

＜鍼先の先鋭化処理＞

W鍼は50μmφの線材を用い、電解エッチングによって先端を針状に尖らせた。その原理を下図に示す。

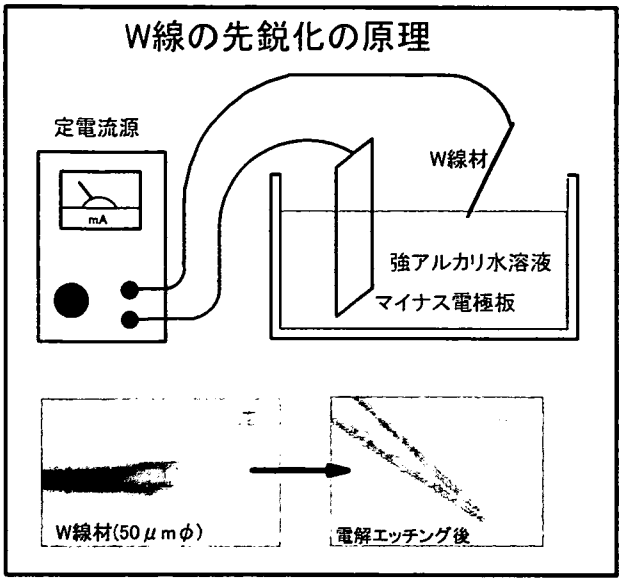

Wの電解エッチング液は、KOH水溶液(40wt%)を用いた。電極板は導通が取れてアルカリに強い金属であれば良いため、Crメッキされた薄い鉄板を使用した。W線に定電流源のプラス極からリード線をワニロクリップなどで接続し、マイナス電極板の入ったKOH水溶液に先端2mm程度を投入し通電する。WはKOH水溶液中にWイオンとして溶解し、先端から細くなり、先鋭化される。反応中は泡が発生する。水溶液から取り出す目安は先端が尖ってくると電圧表示が急に高くなるのでその時点で取り出すとほぼ同じ形状の針が得られる。

＜絶縁被覆＞

W鍼に絶縁膜を形成した。絶縁膜は、撥水性、耐薬品性にも優れて安定な有機膜として医療器具分野、電子回路分野などに広く使われているポリパラキンレン(パリレン)樹脂を使用した。これはCVD(Chemical Vapor Deposition)によるので、分子レベルでのコンフォーマルな膜付けが可能である。プロセスは以下の通りである。

a. 原料ダルマー(粉末・パラキシリレン2量体)を気化室に入れて加熱する。

b. 加熱蒸発したダルマーは、高温の熱分解室に導かれて、ここで反応性の高いラジカルなモノマー(パラキシリレン)になる。

c. ラジカル化した蒸気が蒸着室内で物体に接し、そこで重合して高分子膜(パリレン樹脂膜)を生成する。

下図に、W鍼に5μm厚でCVDしたパリレン膜を鍼先端のみ被覆除去した状態の写真を示す。

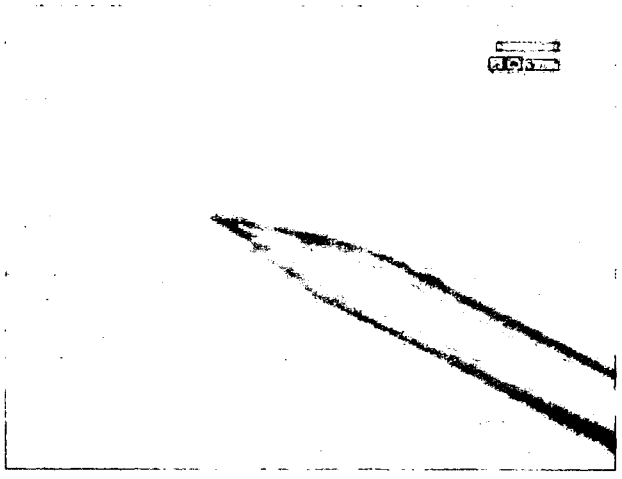

4－1－3．鍼デバイスの製作

鍼デバイスは、Si台座の中央部にパリレンコートW鍼(W線50μmφ，パリレン5μm厚)を挿入固定した鍼部と、同じくSi台座にウレタンコートAu線（Au線60μmφ，ウレタン7.5μm厚）を導通接続した導線部(約15cm)と電極端子（差動アンプとの接続端子）を主な構成部材としている。下図に完成したデバイスの写真を示す。

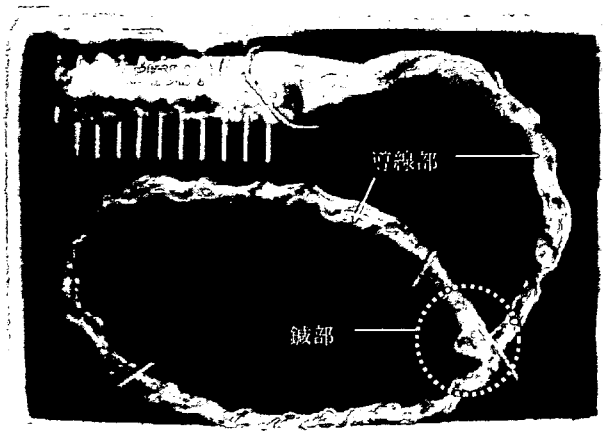

組立て手順の概要を、以下に示す。

（A）W鍼のSiベースへの取り付け （表A）

W鍼は、Si台座表面から、0.3～0.5mm程度突き出るように長さを調整した。またSiベースの鍼受け部にパリレン被覆を除去して根元を90度折り曲げて、Siベースに固定・接着できるようにした。鍼受け部にAgペーストを満たし、～150℃で数分間乾燥・固化により、鍼と後のリード線への電気的導通経路を保ちつつしっかり固定する。

（B）Ａｕ配線の接続と伸縮機構の製作（表B）

ウレタン被覆を約20mm程度除去したAu線を、Siベースの両端に形成したリード線固定孔へ挿入し、孔に巻きつけて仮固定する。次にAgペーストでAu線のあるパッド部全体を満たし、固化させる。乾燥後、Agペーストによる電気的リークがないことを確認し、余分なAu線を取り除き、Si樹脂をSi台座全体に塗布して絶縁を兼ねた保護を兼ねた処理を施す。

次に、図Ｂ　3-①に示すように、神経固定用のSiチューブを準備し、針デバイスを一部をくり抜いたSiチューブへ写真に示したように挿入・接着固定する。最後にチューブの長さを5mm程度にし、神経鞘を投入する切れ目を入れる。

（C）電極分岐端子の接続と固定（表C）

Auワイヤーは、10本のW鍼と電気的にそれぞれ独立接続される必要があるので、電極端子のNo.と鍼の関係が明確である必要がある。このため、Au線1本1本にNo札をつけ、電極端子に順番に接続される。また10本のAu線に伸縮性をもたせるために、Siチューブに螺旋状に巻き付け固定した。Siチューブは、鍼デバイス部のSiチューブと電極端子にしっかり接着固定される。

（D）配線（表D）

マウントベース冶具に対し、Au線の末端を表Dに示す手順で接続して行く。基本的にAgペーストで導通を取り、固定する方法は変わらない。最後にAu線を巻き付けているSiチューブとマウントベースを接着固定し、完成となる。

表A

	大工程	断面鳥瞰図・写真	プロセス・写真
1	W鍼の形成	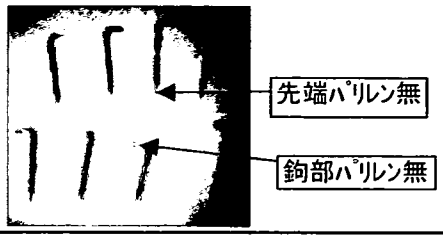	鍼先端のパリレンコートを除去し、先端から400μm～600μmの長さで曲げ曲げたところを150μm程度残してカットし、パリレンも除去する。
2	Si台座アッセンブリ		Si台座断面
	①Agペースト		Agペースト注入
	②鍼挿入	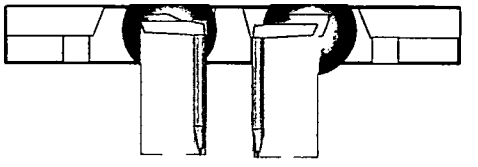	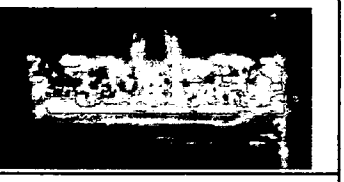
	③Agペースト充填 乾燥・硬貨	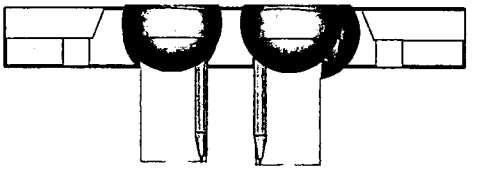 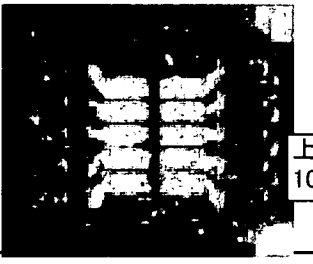	Agペーストで完全に埋込み
	④ Agペースト	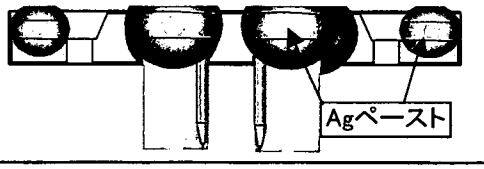	150℃乾燥・固化

表B

	⑤Au線挿入巻付け リード線引き出しパッド部	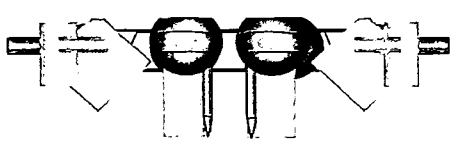	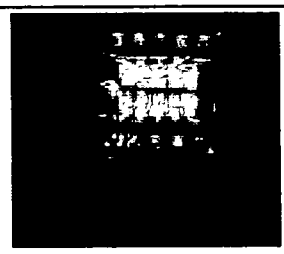
	⑥Agペースト注入	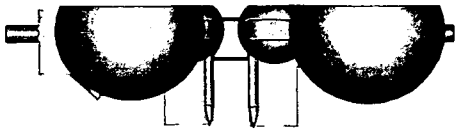 150℃乾燥・固化	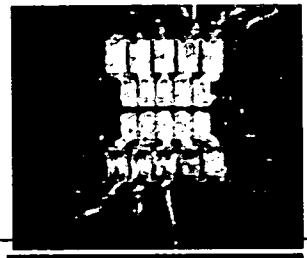
	⑦Au線調整・樹脂被覆	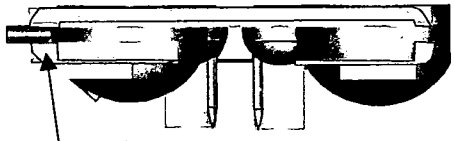 Si樹脂	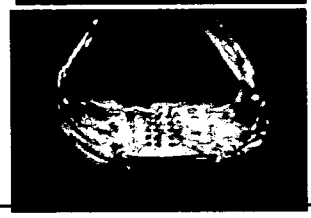
3	神経固定治具形成 ①Siチューブと一体化	 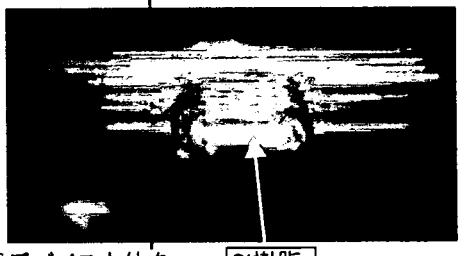 Siチューブ(1×2mmφ or 1.5×2.5mmφ)に穴を開け、鍼デバイス本体をSi樹脂で固定 Si樹脂	
	②神経挿入用の切れ目を入れる		 チューブ孔側から見た状

表C

4 Auワイヤー処理

①鍼とNo.が一致するようにAu線に番号札をつける

1～10まで1枚づつNo.が振ってある

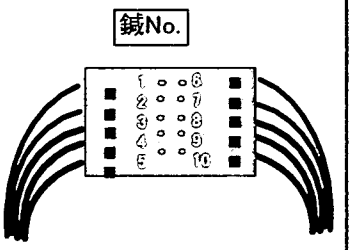

②Auワイヤーを束ねて拠り合わせ1束のリード線とし、Si樹脂を塗って保護する。
更に外径1mmφ程度のSiチューブを少し伸ばした状態で固定し、これにリード線の束を巻きつけ、Si接着材で固定する。固まったら伸ばしていたSiチューブを開放する。リード部は伸縮可能なリード線になっている。リード線は、真直ぐな状態で280mm、Siﾁｭｰﾌﾞに巻き付けた状態で140～150mm程度になる。30～40mmはSiﾁｭｰﾌﾞごと引き伸ばせる構造になっている。

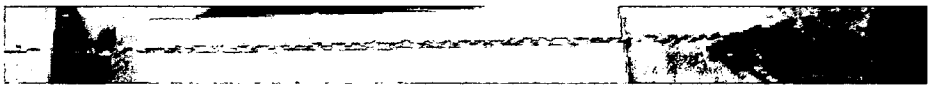

③鍼デバイス部とSiチューブを、エポキシ樹脂及びSi接着剤により固着する。

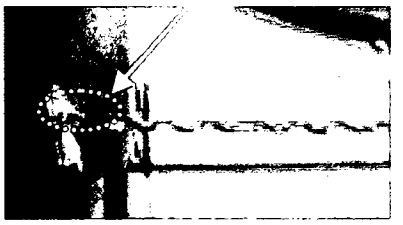

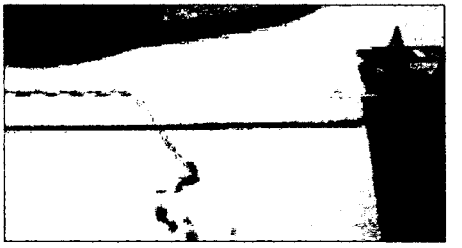

④Au端子と電極端子との接続
※引き出し電極端子として用いたIC電極端子類

IC用マウントベース
16ﾋﾟﾝﾀｲﾌﾟ

IC用マウントベース
12ﾋﾟﾝﾀｲﾌﾟ

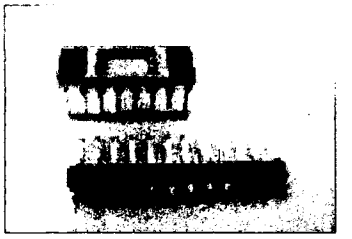

表D

④-1. 配線の仮固定 (ICマウントベース)	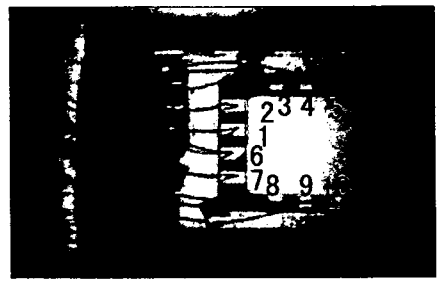	片側の端子5本づつ使用 マウント面の端子パッドへ Au線1本づつテープで仮止め
④-2. Agﾍﾟｰｽﾄ固定 ｴﾎﾟｷｼ樹脂	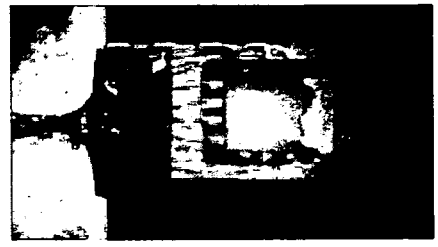	Agペーストで接続し、固化させる エポキシ樹脂で被覆し、更に Si樹脂でベース部分全体を コート
(配線接続ﾀｰﾐﾅﾙ) ⑤-1Au線の巻き付け	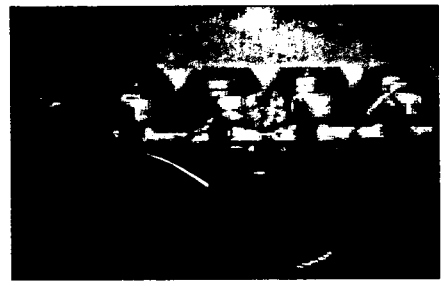	短い端子側にAu線を巻き付ける Agペーストで固定
⑤-2配線固定・まとめ	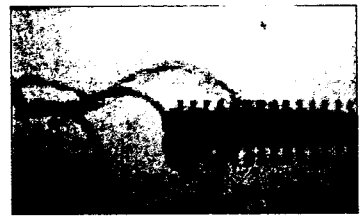	Siチューブを電極端子へ接着
5-③電極端子固定一体化	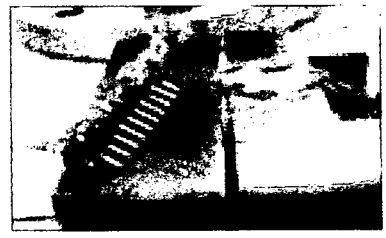	余ったリード線の束をまとめて Siチューブへ巻き付けしっかり 接着・固定
(完成例) 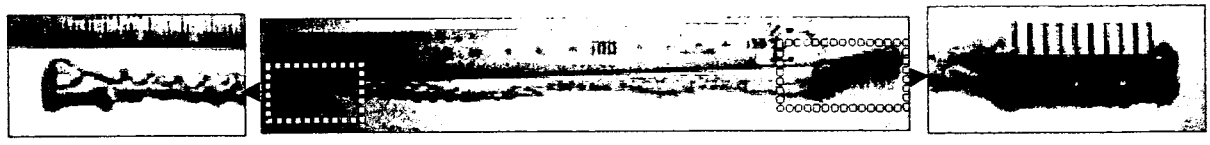		

＜倫理面への配慮＞

本研究の動物実験は、国立循環器病センター研究所および日本生理学学会の動物実験の指針に沿い、実験動物の数と侵襲を最小にするよう、また、動物愛護上においても、十分配慮して行われた。また、国立循環器病センター研究所実験動物委員会に承認のもとに、行われた。

E．研究発表

1．論文発表

1) Uemura K, Li M, Tsutsumi T, Yamazaki T, Kawada T, Kamiya A, Inagaki M, Sunagawa K, Sugimachi M. Efferent vagal nerve stimulation induces tissue inhibitor of metalloproteinase-1 in myocardial ischemia-reperfusion injury in rabbit. Am J Physiol Heart Circ Physiol. 2007 Oct;293(4):H2254-61. PMID: 17693545

2) Mizuno M, Kamiya A, Kawada T, Miyamoto T, Shimizu S, Sugimachi M. Muscarinic potassium channels augment dynamic and static heart rate Responses to vagal stimulation. Am J Physiol Heart Circ Physiol. 2007 Sep;293(3):H1564-70. PMID: 17526651

3) Kawada T, Kitagawa H, Yamazaki T, Akiyama T, Kamiya A, Uemura K, Mori H, Sugimachi M. Hypothermia reduces ischemia- and stimulation-induced myocardial interstitial norepinephrine and acetylcholine releases. J Appl Physiol. 2007 Feb;102(2):622-7. PMID: 17082372

4) Sugimachi M, Kawada T, Kamiya A, Li M, Zheng C, Sunagawa K. Electrical Acupuncture Modifies Autonomic Balance by Resetting the Neural Arc of Arterial Baroreflex System. Conf Proc IEEE Eng Med Biol Soc; 1: 5334-5337, 2007.

2．学会発表

1) 川田　徹、山崎　登自、秋山　剛、宍戸　稔聡、神谷　厚範、水野　正樹、杉町　勝アンジオテンシンⅡは迷走神経刺激時の心筋間質におけるアセチルコリン放出を抑制する　第84回日本生理学会大会　Program2007

2) 水野　正樹、神谷　厚範、川田　徹、杉町　勝 K_{ACh} チャンネルは迷走神経性心拍反応を高速化し倍化する　第84回日本生理学会大会　Program2007

3) 神谷　厚範、上村　和紀、水野　正樹、清水　秀二、杉町　勝　閉胸下臨床医学現場で非代償性重症心不全の血行動態を管理する、新しい自動薬物治療装置　第84回日本生理学会大会　Program2007

4) 水野　正樹、神谷　厚範、川田　徹、杉町　勝　ムスカリン性 K＋チャネルは迷走神経刺激に対する心拍応答を高速化し倍化する　第４６回日本生体工学会大会

5) 清水　秀二、宍戸　稔聡、上村　和紀、神谷　厚範、杉町　勝　Norwood 手術のシャント術式が心臓エナジェティクスに与える影響　第４６回日本生体工学会大会

6) 宮本　忠吉、稲垣　正司、高木　洋、川田　徹、宍戸　稔聡、神谷　厚範、杉町　勝　　ヒト呼吸化学調節系の動特性の定量評価　第４６回日本生体工学会大会

7) 上村　和紀、神谷　厚範、杉町　勝、砂川　賢二　血行動態自動制御システムによる心臓酸素効率最適化　第４６回日本生体工学会大会

8) 神谷　厚範、上村　和紀、水野　正樹、清水　秀二、砂川　賢二　閉胸下臨床医学現で、非代償性重症心不全の血行動態を管理する、自動薬物治療

装置　　第４６回日本生体工学会大会

9) 杉町　勝、李　梅花、鄭　燦、神谷　厚範、川田　徹　電気鍼による動脈圧反射系の修飾とその循環器疾患治療への応用　第４６回日本生体工学会大会

10) 上村　和紀、神谷　厚範、杉町　勝、砂川　賢二　包括的循環平衡モデルの開発とその有用性　第２８回日本循環制御医学会総会

11) 杉町　勝、上村　和紀、神谷　厚範、清水　秀二、宍戸　稔聡、砂川　賢二　包括循環平衡モデルに基づくバイオニック循環管理　第２８回日本循環制御医学会総会

12) T. Kawda, T.Miyamoto, M.Li, A.Kamiya and M.Sugimachi Dynamic characteristics of sympathetic nerve activity response to Electroacupuncture at Zusanli in anesthetized cat. EXRERIMENTAL BIOLOGY 2007

13) M Sugimachi,T Kawada,A Kamiya,M Li,C Zheng,K Sunagawa Electrical Acupuncture Modifies Autonomic Balance by Resetting the Neural Arc of Arterial Baroreflex System. pp.5334-5337 IEEE EMB 2007

14) S Shimizu,T Shishido,K Uemura,A Kamiya,T Kawada,S Sano,M Sugimachi Right ventricle-pulmonary artery shunt for Norwood procedure is beveficial in reducing pressure-volume area and myocardial oxygen consumption compared to Blalock-Taussing Shunt:an in-silico analysis. European Society of Cardiology 2007

15) 水野正樹、神谷厚範、川田徹、宍戸稔聡、杉町勝　ムスカリン性 K+チャネルは交感神経緊張の有無に関わらず迷走神経刺激に対する動的及び静的心拍応答に貢献している　第 85 回日本生理学会総会

16) 川田徹、水野正樹、神谷厚範、宍戸稔聡、杉町勝　血圧フィードバックによる電気鍼を用いた交感神経抑制システムの開発　第 85 回日本生理学会総会

Ｆ．知的財産権の出願・登録状況

１．特許取得

【発明の名称】神経信号用プローバ、神経信号出力装置、神経信号記録装置、神経刺激装置及び神経信号入出力装置

【名称】神経信号用プローバ、神経信号出力装置、神経信号記録装置、神経刺激装置及び神経信号入出力装置

【発明者】神谷厚範、杉町　勝、桜井史敏、慶光院利映

【出願日】平成 19 年 2 月 1 日

【出願番号】特願 2007-023501

２．実用新案登録

なし。

３．その他

なし。

研究成果の刊行に関する一覧表

書籍

なし

雑誌

発表者氏名	論文タイトル名	発表誌名	巻号	ページ	出版年
Uemura K, Li M, Tsutsumi T, Yamazaki T, Kawada T, Kamiya A, Inagaki M, Sunagawa K, Sugimachi M.	Efferent vagal nerve stimulation induces tissue inhibitor of metalloproteinase-1 in myocardial ischemia-reperfusion injury in rabbit.	Am J Physiol Heart Circ Physiol	293	H2254-2261	2007
Sugimachi M, Kawada T, Kamiya A, Li M, Zheng C, Sunagawa K.	Electrical Acupuncture Modifies Autonomic Balance by Resetting the Neural Arc of Arterial Baroreflex System.	Conf Proc IEEE Eng Med Biol Soc	1	5334-5337	2007
Mizuno M, Kamiya A, Kawada T, Miyamoto T, Shimizu S, Sugimachi M.	Muscarinic potassium channels augment dynamic and static heart rate responses to vagal stimulation.	Am J Physiol Heart Circ Physiol	293	H1564-1570	2007
Kawada T, Kitagawa H, Yamazaki T, Akiyama T, Kamiya A, Uemura K, Mori H, Sugimachi M.	Hypothermia reduces ischemia- and stimulation-induced myocardial interstitial norepinephrine and acetylcholine releases.	J Appl Physiol	102	622-627	2007

Am J Physiol Heart Circ Physiol 293: H2254–H2261, 2007.
First published August 10, 2007; doi:10.1152/ajpheart.00490.2007.

Efferent vagal nerve stimulation induces tissue inhibitor of metalloproteinase-1 in myocardial ischemia-reperfusion injury in rabbit

Kazunori Uemura,[1] Meihua Li,[1] Takaki Tsutsumi,[2] Toji Yamazaki,[3] Toru Kawada,[1] Atsunori Kamiya,[1] Masashi Inagaki,[1] Kenji Sunagawa,[2] and Masaru Sugimachi[1]

Departments of [1]Cardiovascular Dynamics and [3]Cardiac Physiology, National Cardiovascular Center Research Institute, Suita, Japan; and [2]Department of Cardiovascular Medicine, Kyushu University Graduate School of Medical Science, Fukuoka, Japan

Submitted 24 April 2007; accepted in final form 7 August 2007

Uemura K, Li M, Tsutsumi T, Yamazaki T, Kawada T, Kamiya A, Inagaki M, Sunagawa K, Sugimachi M. Efferent vagal nerve stimulation induces tissue inhibitor of metalloproteinase-1 in myocardial ischemia-reperfusion injury in rabbit. *Am J Physiol Heart Circ Physiol* 293: H2254–H2261, 2007. First published August 10, 2007; doi:10.1152/ajpheart.00490.2007.—Vagal nerve stimulation has been suggested to ameliorate left ventricular (LV) remodeling in heart failure. However, it is not known whether and to what degree vagal nerve stimulation affects matrix metalloproteinase (MMP) and tissue inhibitor of MMP (TIMP) in myocardium, which are known to play crucial roles in LV remodeling. We therefore investigated the effects of electrical stimulation of efferent vagal nerve on myocardial expression and activation of MMPs and TIMPs in a rabbit model of myocardial ischemia-reperfusion (I/R) injury. Anesthetized rabbits were subjected to 60 min of left coronary artery occlusion and 180 min of reperfusion with (I/R-VS, $n = 8$) or without vagal nerve stimulation (I/R, $n = 7$). Rabbits not subjected to coronary occlusion with (VS, $n = 7$) or without vagal stimulation (sham, $n = 7$) were used as controls. Total MMP-9 protein increased significantly after left coronary artery occlusion in I/R-VS and I/R to a similar degree compared with VS and sham values. Endogenous active MMP-9 protein level was significantly lower in I/R-VS compared with I/R. TIMP-1 mRNA expression was significantly increased in I/R-VS compared with the I/R, VS, and sham groups. TIMP-1 protein was significantly increased in I/R-VS and VS compared with the I/R and sham groups. Cardiac microdialysis technique demonstrated that topical perfusion of acetylcholine increased dialysate TIMP-1 protein level, which was suppressed by coperfusion of atropine. Immunohistochemistry demonstrated a strong expression of TIMP-1 protein in cardiomyocytes around the dialysis probe used to perfuse acetylcholine. In conclusion, in a rabbit model of myocardial I/R injury, vagal nerve stimulation induced TIMP-1 expression in cardiomyocytes and reduced active MMP-9.

myocardial remodeling; matrix metalloproteinase; acetylcholine

LEFT VENTRICULAR (LV) myocardial remodeling that occurs after myocardial infarction (MI) leads to progressive LV dilation and eventually pump dysfunction (33, 40). In addition to the loss of contractile cardiomyocytes, pathological degradation and reconstitution of extracellular matrix significantly contribute to the progression of LV remodeling, where matrix metalloproteinase (MMP) and its intrinsic inhibitor, tissue inhibitor of MMP (TIMP), play crucial roles (37, 43).

A previous study using genetically engineered mice demonstrated that target deletion of the MMP-9 gene prevented LV rupture and ameliorated LV remodeling after MI (10). The positive results of MMP inhibition on LV remodeling in animal models led to the proposal to use MMP inhibitors as a potential therapy for patients at risk for the development of heart failure after MI (27, 32). However, recent clinical results from the Prevention of Myocardial Infarction Early Remodeling (PREMIER) trial failed to demonstrate a beneficial effect of MMP inhibition on LV remodeling after MI (16). This indicates the importance of further understanding the in vivo regulatory mechanisms of MMPs to understand and beneficially modify the LV remodeling process.

The cardiac autonomic nervous system plays an important role in the progression of heart failure (21). A previous communication from our laboratory demonstrated that chronic electrical stimulation of vagal nerve ameliorated LV remodeling and markedly improved survival after MI in rat (23). However, it is not known whether and to what degree the vagal nerve affects the MMPs and the TIMPs in vivo. We therefore investigated the effects of electrical stimulation of vagal nerve on myocardial expression of MMP-2/9 and TIMP-1/2 in a rabbit model of myocardial ischemia-reperfusion (I/R) injury. We also investigated the direct action of acetylcholine (ACh), a neurotransmitter released by vagal nerve stimulation (VNS), on myocardial release of TIMP-1 using a cardiac microdialysis technique (19). Our results indicated that VNS induced expression of TIMP-1 from cardiomyocytes and reduced active MMP-9 in myocardial I/R injury in rabbit.

METHODS

We used 49 Japanese white rabbits in this study (male, 2.5–3.0 kg). Care of the animals was in strict accordance with the guiding principles of the Physiological Society of Japan. All protocols were approved by the Animal Subjects Committee of the National Cardiovascular Center.

I/R Study

Experimental preparation. Anesthesia was induced by intravenous injection of pentobarbital sodium (35 mg/kg). Animals were tracheotomized, intubated, and mechanically ventilated. Arterial pH, P_{O_2}, and P_{CO_2} were maintained within the physiological ranges by supplying oxygen and changing the respiratory rate. α-Chloralose (20 $mg \cdot kg^{-1} \cdot h^{-1}$) was continuously infused to maintain an appropriate level of anesthesia during the experiment. A catheter-tipped micromanometer (SPC-330A, Millar Instruments, Houston, TX) was inserted via the right femoral artery to measure arterial pressure (AP). After a median sternotomy, the heart was suspended in a pericardial

Address for reprint requests and other correspondence: K. Uemura, Dept. of Cardiovascular Dynamics, National Cardiovascular Center Research Inst., 5-7-1 Fujishirodai, Suita 565-8565, Japan (e-mail: kuemura@ri.ncvc.go.jp).

The costs of publication of this article were defrayed in part by the payment of page charges. The article must therefore be hereby marked "*advertisement*" in accordance with 18 U.S.C. Section 1734 solely to indicate this fact.

cradle. Another catheter-tipped micromanometer was introduced into the LV via the apex to measure LV pressure (LVP). Piezoelectric crystals (1 mm, Sonometrics, Ontario, Canada) were attached to the anterior and lateral walls of the LV using cyanoacrylate adhesive (3M, Vetbond, St. Paul, MN) to measure regional LV segmental length. A 4-0 proline suture was passed around the main branch of the left anterior descending coronary artery (LAD), and a snare was formed by passing the ends of the thread through a small vinyl tube. A surface electrocardiogram (ECG) was recorded.

Bilateral cervical vagi were identified and transected at the neck region. A pair of bipolar electrodes was attached at the cardiac end of the right vagal nerve. The duration of electrical pulse used to stimulate the vagal nerve was set at 4 ms. We adjusted the amplitude of the pulse in each animal to reduce heart rate (HR) by 30% from the baseline value at a stimulation frequency of 10 Hz. The resultant stimulation voltage was 2–4 V.

Experimental protocol. Thirty minutes were allowed for stabilization after the initial preparation and surgical procedures were completed. The animals were randomized into the following four groups: *1*) sham group (n = 7), in which surgical preparation was conducted without coronary occlusion or vagal stimulation (VS); *2*) VS group (n = 7), in which stimulation of the vagal nerve was started after baseline hemodynamics were obtained and continued during the experiment; *3*) I/R group (n = 7), in which 60 min of LAD occlusion and 180 min of reperfusion were conducted; and *4*) I/R-VS group (n = 8), in which stimulation of the vagal nerve was started 15 min before LAD occlusion and continued throughout 60 min of myocardial ischemia and 180 min of reperfusion.

Baseline hemodynamic data (baseline) were recorded in all groups. A second set of measurements of hemodynamic data (60 min) was obtained during the last 5 min of the 60-min observation period in the sham and VS groups or during the last 5 min of the 60-min ischemic period in the I/R and I/R-VS groups. A third set of measurements of hemodynamic data (240 min) was recorded during the last 5 min of the next 180-min observation period in the sham and VS groups or during the last 5 min of the 180-min reperfusion period in the I/R and I/R-VS groups.

At each time point, hemodynamic data were recorded under a steady-state condition. All data acquisitions were done at end expiration. Analog signals of AP, LVP, segmental length of the anterior-lateral wall of LV (risk area), and ECG were digitized at 200 Hz and stored in a computer for off-line analysis (Sonolab, Sonometrics).

At the end of the experiment, the animal was euthanized. The whole heart was quickly excised and washed with cold PBS. After the vasculature, right ventricular free wall, and atrial appendages were dissected away, the remaining LV wall was snap frozen in liquid nitrogen and stored at −80°C.

Myocardial protein extraction. Approximately 200 mg of myocardial tissue sample obtained from the center of the risk area (anterior wall) of the LV free wall was homogenized in 1 ml of lysis buffer containing 50 mmol/l Tris (pH 7.4), 1.5 mmol/l $CaCl_2$, and 0.5% Triton X-100. The homogenate was centrifuged at 2,000 *g* for 10 min at 4°C, and the supernatant was collected. Protein concentration of each supernatant sample was determined with a DC Protein assay kit (Bio-Rad, Richmond, CA).

Gelatin zymography. Gelatin zymography was performed to assess the relative contents of the gelatinases MMP-2 and MMP-9 (43). The supernatants (60 μg protein) were loaded in Novex precast 10% Tris-glycine gels containing 0.1% gelatin (Invitrogen, Carlsbad, CA) and then electrophoresed. After renaturation and equilibration, the gels were incubated for 30 h at 37°C in Novex zymogram-developing buffer. The gels were then stained in 0.5% Coomassie blue G-250, dissolved in 30% methanol-10% acetic acid for 60 min, and destained in several changes of methanol-acetic acid for 60 min. Gels were dried and scanned. MMP-2 and MMP-9 related bands were analyzed using the NIH Image software (ImageJ 1.37).

MMP-9 activity assay. Bioactivity assay for MMP-9 was performed using the Biotrak activity assay system (GE Healthcare Bio-Sciences, Piscataway, NJ) following the manufacturer's instructions (42). Briefly, supernatant samples were placed in microtitre well plates coated with anti-MMP-9 (100 μl/well). The plates were incubated overnight at 4°C. The following day, *p*-aminophenylmercuric acetate was added to the wells for measuring "total" MMP-9 (pro- and active MMP-9). Buffer alone was added to the wells for measuring "active" (endogenous active MMP-9) MMP-9. Detection agent was then added to all wells (50 μl/well), and the plate was read at 405 nm (t = 0 min) and again after a 2-h incubation at 37°C. The value of MMP-9 was standardized by the protein concentration. All measurements were run in duplicate.

ELISA measurement of TIMP-1 and TIMP-2. Commercially available ELISA kits (Daiichi Fine Chemical, Toyama, Japan) were used to measure TIMP-1 and TIMP-2 levels in supernatants according to the manufacturer's instructions (13, 17, 20). Briefly, standards and samples were incubated in microtitre wells coated with anti-TIMP-1 and anti-TIMP-2 antibody. Peroxidase-labeled antibodies directed to the respective TIMPs were added to the corresponding wells. Visualization of the presence of the peroxidase label was achieved using the *o*-phenylenediamine substrate (TIMP-1) or tetramethylbenzidine substrate (TIMP-2). The plates were read at 490 (TIMP-1) or 450 (TIMP-2) nm. Values of TIMPs were standardized by the protein concentration. Since the ELISA systems have some degree of intraplate and interplate variability (<15%) (7), all measurements were run in duplicate to quadruplicate.

Myocardial RNA extraction and reverse transcription. Total RNA was extracted from the risk area (anterior wall) of the LV free wall by an acid guanidium thiocyanate-phenol chloroform method (Isogen, Nippon Gene). First-strand cDNA was synthesized using reverse transcriptase with random hexamer primers from 1 μg of total RNA in a final volume of 20 μl, according to the manufacturer's protocol (ReverTra Ace, Toyobo).

Real-time quantitative reverse transcription-PCR. To analyze TIMP-1 gene expression in myocardial tissue, real-time polymerase chain reaction (PCR) amplification was performed with SYBR Premix Ex Taq (Perfect Real Time; TaKaRa, Japan) using the ABI PRISM 7500 sequence detection system (Applied Biosystems). For standardization and quantification, rabbit glyceraldehyde 3-phosphate dehydrogenase (GAPDH) was amplified simultaneously. The respective PCR primers were designed from GenBank databases (Table 1). The PCR consisted of initial treatments (50°C, 2 min; and 95°C, 10 min) followed by 40 three-step cycles (denaturation 94°C, 10 s; annealing 60°C, 10 s; and extension 72°C, 40 s). Fluorescence was detected at the end of every extension phase (72°C). After PCR amplification, dissociation curves were constructed to confirm the formation of the intended PCR products. Relative expression of TIMP-1 to the GAPDH levels was calculated as described previously (28, 45).

Hemodynamic data analysis. The following hemodynamic parameters were determined from hemodynamic data: HR, mean arterial pressure, maximum first derivative of LVP (LV dP/dt_{max}), and fractional shortening of anterior-lateral wall (FS). End diastole and end ejection were defined as the peak of R wave of ECG and the peak of minimum first derivative of LVP, respectively. FS was calculated as

Table 1. *Probes used for real-time PCR*

Assay	Sequence	Accession Number
TIMP-1		
Forward	5′-CAACTCCGACCTTGTCATCAG-3′	AY829731
Reverse	5′-GCGTCAAATCCTTTGAACATCT-3′	
GAPDH		
Forward	5′-GGAGAAAGCTGCTAAGTATGACG-3′	L23961
Reverse	5′-CACTGTTGA AGTCGCAGGAG-3′	

TIMP-1, tissue inhibitor of matrix metalloproteinase-1.

the ratio of systolic stroke change in segmental length and end-diastolic length of the anterior-lateral wall (36).

Cardiac Microdialysis Study

Experimental preparation. Experimental preparation was the same as described above in *I/R Study*, except that no coronary artery occlusion was performed. A microdialysis probe was implanted into the LV anterior wall. Heparin sodium (200 U/kg) was administered intravenously to prevent blood coagulation (19).

Dialysis technique. The materials and properties of the dialysis probe have been described (19). Briefly, we designed a hand-made long transverse dialysis probe. One end of a polyethylene tube (25 cm long, 0.5 mm OD, and 0.2 mm ID) was dilated with a 27-gauge needle (0.4 mm OD). Each end of the dialysis fiber (8 mm long, 0.215 mm OD, 0.175 mm ID, and 300 Å pore size; Evaflux type 5A, Kuraray Medical, Tokyo, Japan) was inserted into the polyethylene tube and glued.

Recovery of TIMP-1 passing through the dialysis fiber membrane was evaluated in vitro. The dialysis probe ($n = 4$) was immersed in Ringer solution (in mM; 147.0 NaCl, 4.0 KCl, and 2.25 $CaCl_2$) containing Tween 20 (0.1%) and various concentrations of TIMP-1 (10–40 ng/ml, free form of human TIMP-1, Daiichi Fine Chemical). The dialysis probe was perfused with Ringer solution at a rate of 2.5 μl/min using a microinjection pump (model CMA/102, Carnegie Medicine). We measured the concentration of TIMP-1 in the dialysate sample using an ELISA kit. The relative recovery of TIMP-1 was calculated as the ratio of TIMP-1 concentration in dialysate to its concentration in the medium surrounding the probe (11, 22). The relative recovery of TIMP-1 was 11.1 ± 0.3%. Recovery was constant between probes and within the probe for the TIMP-1 concentration range studied.

A fine-guiding needle (25 mm long, 0.51 mm OD, and 0.25 mm ID) was used for implantation of the dialysis probes. The guiding needle was connected to the dialysis probe with a stainless steel rod (5 mm long and 0.25 mm OD). Experimental protocols were initiated 2 h after implanting the dialysis probe. The dialysate sampling period was set at 60 min and was performed taking into account the dead space volume between the dialysis membrane and the sample tube.

Experimental protocol. After baseline dialysate was sampled and baseline hemodynamic data were recorded, the animals were randomized into the following three groups: *1*) VNS group ($n = 5$), in which electrical stimulation of vagal nerve was performed while the LV wall was perfused with Ringer solution via the dialysis probe; *2*) ACh group ($n = 8$), in which the LV wall was perfused with Ringer solution containing ACh (1 mM); and *3*) ACh-atropine (Atr) group ($n = 7$), in which the LV wall was perfused with Ringer solution containing ACh (1 mM) and Atr (0.2 mM). At 150 min after randomization, dialysate sampling and hemodynamic data recording were performed.

At the end of the experiment, the animal was euthanized. From selected hearts, transmural blocks of the LV free wall containing the dialysis probe were fixed in 4% paraformaldehyde for immunohistochemistry.

Immunohistochemistry and confocal microscopy. To investigate the distribution of TIMP-1, we performed confocal image analysis of LV tissue stained with anti-TIMP-1 antibody. Fixed blocks of LV tissues were washed in 0.1 mol/l phosphate buffer (pH 7.4), embedded in paraffin, and sectioned at a thickness of 5 μm. Sections were deparaffinized using xylene, rehydrated with serial grades of ethanol, and followed by hydration with distilled water. For antigen retrieval of TIMP-1 protein, specimens were immersed in a vessel filled with Target Retrieval Solution (pH 6.1; DAKO). The vessel containing the specimens was autoclaved at 121°C for 20 min. The slides were then allowed to cool at room temperature for 20 min to complete antigen unmasking. The sections were then incubated for 30 h with a mouse anti-TIMP-1 antibody (7-6C1, Daiichi Fine Chemical) diluted 1:5 and then incubated for 2 h in Alexa-488-conjugated goat anti-mouse Ig-G (Molecular Probes) diluted 1:200. Fluorescence of Alexa-488 was observed with a confocal laser-scanning microscope system (FV 300, Olympus). Reconstructed projection images were obtained from serial optical sections recorded at an interval of 0.5 μm.

Exclusion Criteria

Animals were excluded from the study when the following criteria were met: *1*) in the I/R study, coronary artery occlusion did not produce substantial regional dysfunction (FS of the risk area after occlusion was not <20% of the baseline value); *2*) intractable ventricular fibrillation or atrial tachycardia occurred; and *3*) the animal died during the surgical procedure, and the protocol was not completed.

Statistical Analysis

All data are presented as means ± SE. Tukey-Welsch's step-down multiple comparison test was used to determine the significance of differences among groups. P values <0.05 were considered statistically significant.

RESULTS

I/R Study

As shown in Fig. 1*A*, zymography of the myocardial extracts detected two bands at 92 and 72 kDa, corresponding to MMP-9 and MMP-2, respectively. Densitometric analysis demonstrated that relative MMP-9 level increased to a similar degree in the I/R and I/R-VS groups compared with the sham and VS groups (Fig. 1*B*). The relative MMP-2 level decreased in the I/R group compared with the sham and I/R-VS groups (Fig. 1*C*).

Bioactivity assays demonstrated that myocardial levels of total MMP-9 protein increased to a similar degree in the I/R and I/R-VS groups compared with sham and VS groups (Fig. 2*A*). Levels of endogenous active MMP-9 protein also increased in the I/R and I/R-VS groups compared with the sham and VS groups (Fig. 2*B*). The level of active MMP-9 in the I/R-VS group was significantly lower than that in the I/R group (<50%, $P < 0.01$).

The myocardial level of TIMP-1 protein increased in the VS and I/R-VS groups compared with the sham and I/R groups (Fig. 3*A*). There was no significant difference in the myocardial level of TIMP-2 protein among the four groups (Fig. 3*B*). TIMP-1 mRNA as measured by real-time RT-PCR was increased in the I/R-VS group compared with the sham, VS, and I/R groups (Fig. 3*C*).

Table 2 summarizes the data of systemic hemodynamics and LV function during the I/R study. In the VS and I/R-VS groups, HR decreased significantly compared with sham and I/R values at 60 and 240 min. In the I/R and I/R-VS groups, FS was depressed during ischemia with only partial recovery after reperfusion. In the I/R and I/R-VS groups, sonomicrometry demonstrated early systolic bulging of the anterior LV wall during ischemia as reflected by negative FS at the 60-min time point. There was no significant difference in LV dP/dt_{max} and FS between the I/R and I/R-VS groups at 60 and 240 min.

Cardiac Microdialysis Study

Figure 4 presents dialysate TIMP-1 concentrations in response to electrical stimulation of the vagal nerve, to perfusion of ACh, and to perfusion of ACh with Atr. There were no

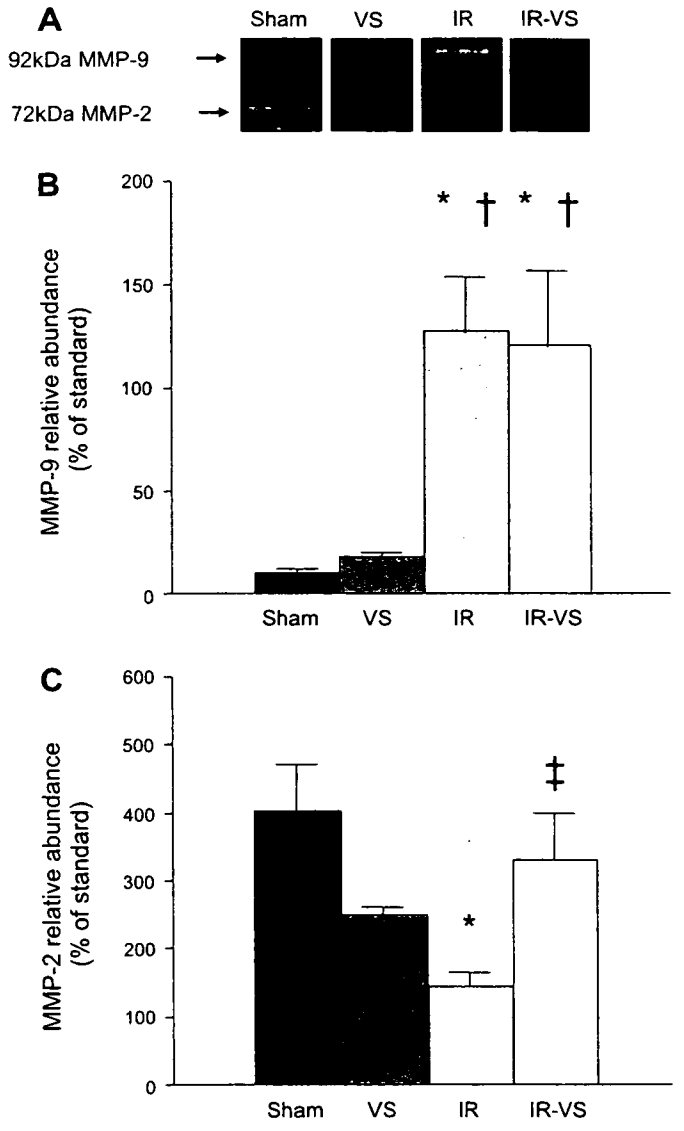

Fig. 1. Zymographic analysis of matrix metalloproteinase (MMP)-9 and -2 proteins in isolated myocardium. Sham, no myocardial ischemia and no vagal stimulation; VS, no myocardial ischemia with vagal stimulation; I/R, myocardial ischemia-reperfusion; I/R-VS, myocardial ischemia-reperfusion with VS. *A*: representative zymogram showing MMP-9 at 92 kDa and MMP-2 at 72 kDa. *B*: densitometric analysis of relative MMP-9 content expressed as percentage of standard. *C*: densitometric analysis of relative MMP-2 content expressed as percentage of standard. Data are means ± SE. *$P < 0.01$ vs. sham; †$P < 0.01$ vs. VS; ‡$P < 0.05$ vs. I/R.

significant differences in baseline TIMP-1 concentrations among the three groups. At 150 min, dialysate TIMP-1 concentration was significantly higher in the VNS and ACh groups than in the ACh-Atr group ($P < 0.05$).

Figure 5 depicts representative microscopic findings of LV tissue around the microdialysis probes in the VNS, ACh, and ACh-Atr groups. Hematoxylin-eosin-stained sections demonstrated only a minimum hemorrhage around the dialysis probe (Fig. 5, *A–C*). TIMP-1-positive cardiomyocytes were detected sparsely but in diffuse distribution throughout the myocardium in the VNS group (Fig. 5*D*). TIMP-1-positive cardiomyocytes were detected over a relatively wide area around the dialysis probe in the ACh group (Fig. 5*E*). TIMP-1-positive cardiomyocytes were also detected but localized close to the dialysis probe in the ACh-Atr group (Fig. 5*F*). Immunoreactive signals of TIMP-1 were restricted to the cytoplasm of cardiomyocytes in all the groups (Fig. 5, *G–I*).

Table 3 summarizes the data of systemic hemodynamics and LV function during the cardiac microdialysis study. In the VNS group, HR decreased significantly compared with that in the ACh and ACh-Atr groups at 150 min. In the ACh and ACh-Atr groups, topical perfusion of ACh or ACh with Atr did not affect the systemic hemodynamics and the LV functions. Except for HR, there were no significant differences in other hemodynamic parameters among the three groups.

DISCUSSION

The major new findings of the present study were as follows. In ischemia-reperfused myocardium, stimulation of the efferent vagal nerve increased TIMP-1 mRNA and protein levels and reduced endogenous active MMP-9 protein. In normal myocardium, VNS or topical perfusion of ACh through a microdialysis probe increased dialysate TIMP-1 protein level. An increase in the dialysate TIMP-1 protein level induced by ACh perfusion was suppressed by coperfusion of Atr.

The robust increase in total MMP-9 levels after reperfusion in this study (Figs. 1*B* and 2*A*) might be mainly due to the

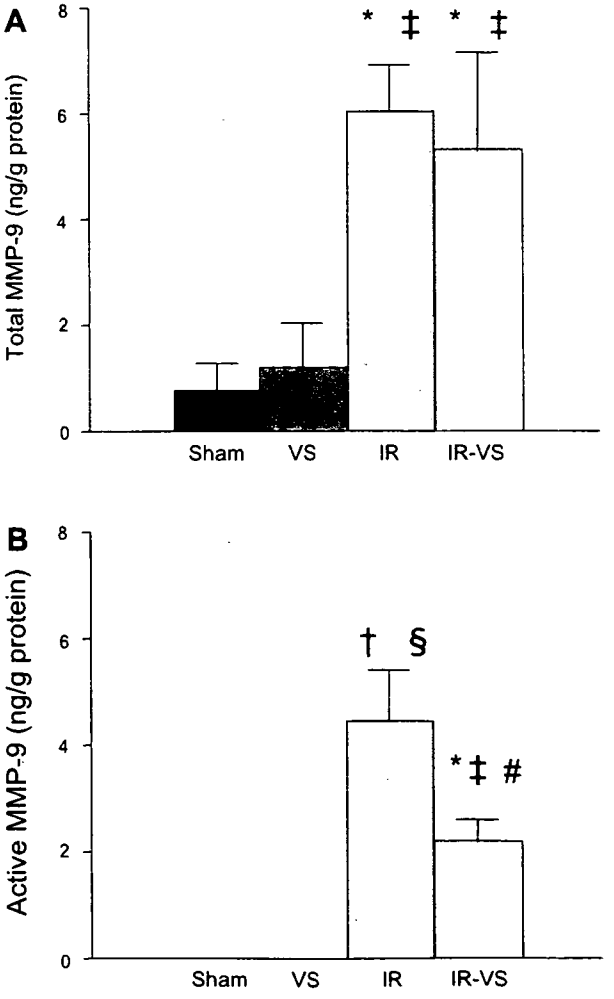

Fig. 2. Bioactivity assay of total (*A*) and active (*B*) MMP-9 protein. *$P < 0.05$; †$P < 0.01$ vs. sham; ‡$P < 0.05$; §$P < 0.01$ vs. VS. #$P < 0.01$ vs. I/R.

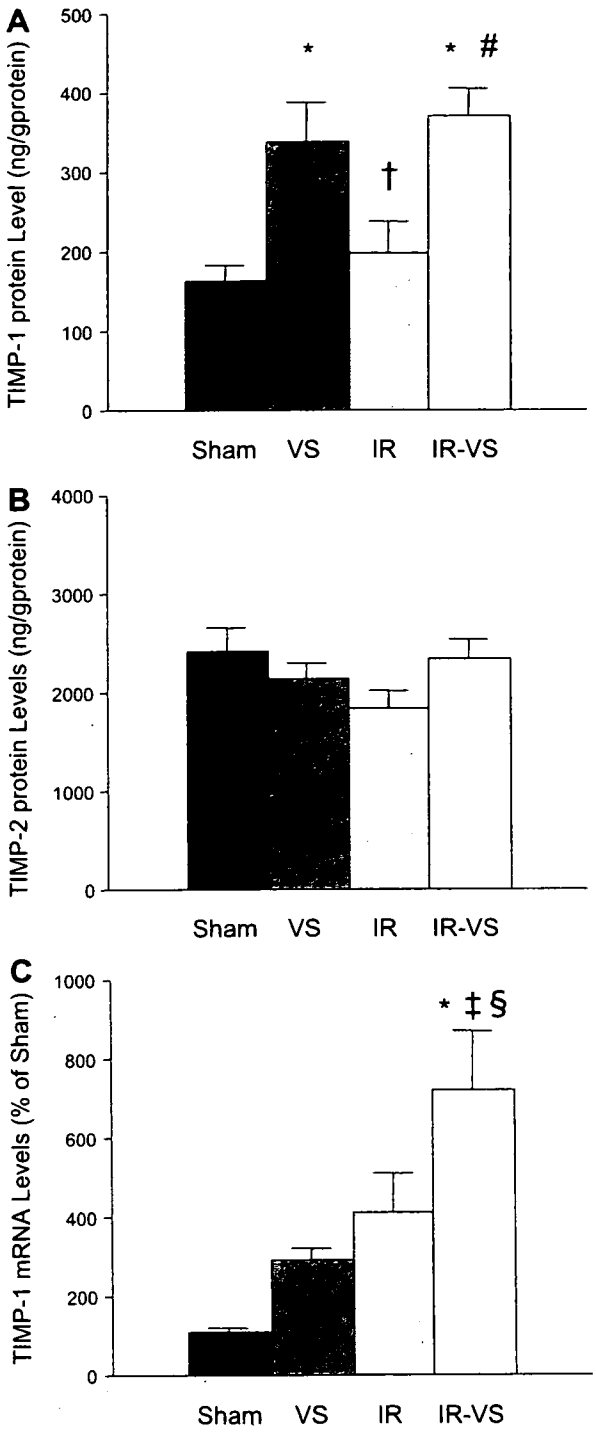

Fig. 3. ELISA measurement of tissue inhibitor of MMP (TIMP)-1 (*A*) and -2 (*B*) protein. Real-time RT-PCR analysis of TIMP-1 mRNA expressed as percentage of sham (*C*). *$P < 0.01$ vs. sham; †$P < 0.05$; ‡$P < 0.01$ vs. VS; §$P < 0.05$; #$P < 0.01$ vs. I/R.

infiltrated neutrophils. Although all cell types, including cardiomyocytes (25, 34) and endothelial cells (41), express MMP-9, neutrophil is an important source of MMP-9 after I/R (26). The level of endogenous active MMP-9 was lower in the I/R-VS group than in the I/R group (Fig. 2*B*). Increased expression of TIMP-1 by VNS (Fig. 3) likely inhibited the conversion of pro-MMP-9 to active MMP-9 and/or inhibited

Table 2. *Hemodynamic parameters during I/R study*

	Baseline	60 min	240 min
HR, beats/min			
Sham	317±9	334±7	326±9
VS	281±14	215±17*‡	238±19*‡
I/R	306±9	316±9	314±8
I/R-VS	301±7	217±5*‡	228±8*‡
MAP, mmHg			
Sham	92±3	93±4	92±3
VS	98±4	91±5	89±5
I/R	102±3	95±4	88±6
I/R-VS	99±4	88±4	83±2
LV dP/dt_{max}, mmHg/s			
Sham	5,119±263	5,308±388	4,819±339
VS	5,040±381	3,993±319	4,140±302
I/R	5,524±423	5,276±404	4,514±467
I/R-VS	5,672±360	4,549±250	4,079±188
FS, %			
Sham	10.8±0.9	10.1±1.0	9.3±1.0
VS	12.2±1.1	11.1±1.2	10.4±1.6
I/R	8.7±0.8	−0.6±0.6*†	0.1±0.8*†
I/R-VS	8.5±1.3	−0.6±0.4*†	1.5±0.7*†

Values are means ± SE. Sham group, no myocardial ischemia and no vagal stimulation (VS); VS group, no myocardial ischemia with VS; I/R group, myocardial ischemia-reperfusion (I/R); IR-VS, myocardial I/R with VS; HR, heart rate; MAP, mean arterial pressure; LV dP/dt_{max}, maximum first derivative of left ventricular (LV) pressure; FS, fractional shortening of anterior wall (risk area). *$P < 0.01$ vs. sham; †$P < 0.01$ vs. VS; ‡$P < 0.01$ vs. I/R.

active MMP-9 itself more potently than in the case without VNS (14). Oxygen free radical induces expression and activation of MMP-9 (17, 41). Reduction of HR by VNS probably reduced myocardial oxygen consumption, ameliorated myocardial ischemia, and reduced oxygen free radicals (30). This may contribute to some extent to the reduction of active MMP-9 in the I/R-VS group.

In the I/R study, TIMP-1 mRNA was significantly higher in the I/R-VS group compared with the sham, VS, and I/R groups (Fig. 3*C*). TIMP-1 mRNA appeared higher in the VS and I/R groups compared with the sham group, although the differences were not significant. Stapel et al. (38) noted increased expression of TIMP-1 mRNA after myocardial I/R in mice. Proinflammatory cytokines such as interleukin-1β induced by

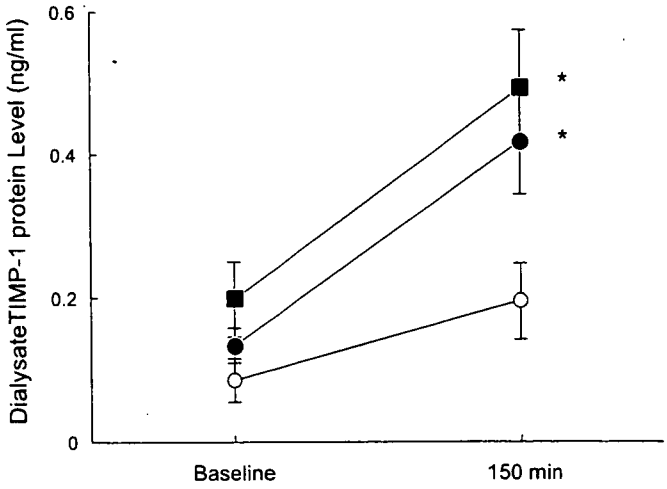

Fig. 4. Dialysate TIMP-1 protein concentration in response to vagal nerve stimulation (■), perfusion of acetylcholine (ACh; ●), or ACh with atropine (Atr) (○). *$P < 0.05$ vs. perfusion of ACh with Atr.

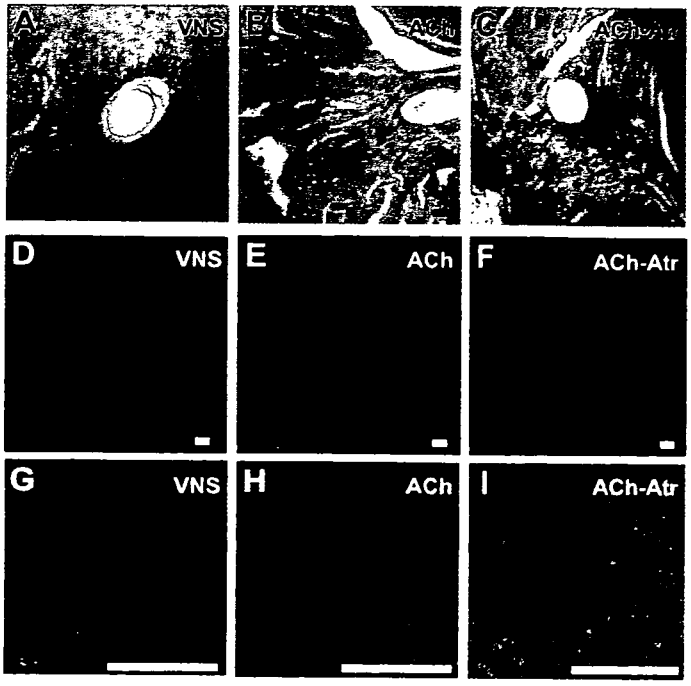

Fig. 5. Representative microscopic finding of left ventricular (LV) tissue implanted with microdialysis probe. *A–C*: hematoxylin and eosin-stained section of LV tissue perfused with Ringer solution under vagal nerve stimulation (VNS; *A*), perfused with ACh (*B*), and perfused with ACh and Atr (ACh-Atr; *C*). *D–F*: anti-TIMP-1 antibody (green)-immunostained sections of LV tissue perfused with Ringer solution under VNS (*D*), perfused with ACh (*E*), and perfused with ACh-Atr (*F*). *G–I*: higher magnifications of *D–F*, respectively. Arrows indicate dialysis probes. Bar = 100 μm.

myocardial ischemia are known to induce TIMP-1 (4). VNS and myocardial ischemia likely exerted an additive effect on the induction of TIMP-1 mRNA in the I/R-VS group. TIMP-1 protein levels in the VS and I/R-VS groups were significantly elevated compared with the sham and I/R groups (Fig. 3*A*). Figure 3, *A* and *C*, indicates dissociation between TIMP-1 mRNA and protein synthesis among the four groups. If the TIMP-1 protein level had correlated with the mRNA level, TIMP-1 protein level in the I/R and I/R-VS groups should have been higher than those presented in Fig. 3*A*. In myocardial ischemia, protein synthesis decreases owing to the inhibition of peptide chain elongation (8, 18). This may have partially inhibited TIMP-1 protein synthesis in the I/R and I/R-VS groups.

In the cardiac microdialysis study, the ACh-induced release of TIMP-1 was mediated by muscarinic ACh receptors because Atr blocked the increase in TIMP-1 in response to ACh stimulation (Fig. 4). TIMP-1 was produced by cardiomyocytes (Fig. 5, *G–I*). These findings suggest that VNS may induce TIMP-1 mRNA expression through muscarinic ACh receptors in cardiomyocytes and increase TIMP-1 protein content in myocardium. The distribution of TIMP-1-positive cardiomyocytes was different among the three groups (Fig. 5, *D–F*). This may reflect differences in the distribution of ACh among the three groups. ACh probably had a diffuse distribution in the myocardium in the VNS group but was concentrated around the dialysis probe in ACh group, whereas the effect of ACh concentrated around the dialysis probe was antagonized by Atr in the ACh-Atr group.

In addition to cardiomyocytes (25, 34), a variety of cell types, such as fibroblasts (14) and endothelial cells (6), produces and secretes TIMP-1. TIMP-1 expression in these cell types is low in the basal condition but is transcriptionally induced by various agents, including the cytokines, serum, growth factors, and phorbol esters (14). The signal transduction pathway from muscarinic ACh receptor stimulation to the induction of the TIMP-1 gene is not clear. Further elucidation of this is not in the scope of this study. ACh increases the production of nitric oxide from cardiomyocytes (9). Nitric oxide induces TIMP-1 gene expression by activating the transforming growth factor-β/Smad signaling pathway in glomerular mesangial cells in the kidney (2). These mechanisms may be involved in the increases in TIMP-1 mRNA and protein induced by VNS in myocardial I/R observed in the present study. Further studies are clearly required to elucidate these issues.

Myocardial expression of TIMP-2 was not modified by VNS (Fig. 3*B*). Contrary to the highly responsive nature of TIMP-1 expression to stimuli, TIMP-2 expression is, for the most part, constitutive (14). Previous studies demonstrated that ischemic injury or change in loading condition had little effect on myocardial expression of TIMP-2 (24, 25, 29). Myocardial content of MMP-2 decreased after I/R, and the decrease was inhibited by VNS (Fig. 1*C*). Cheung et al. (5) demonstrated that MMP-2 was released from the myocardium into the coronary effluent following myocardial I/R, resulting in the depletion of myocardial content of MMP-2.

In the present study, VNS did not prevent contractile dysfunction after I/R (Table 2). Actions of MMP and TIMP did not seem to be responsible for acute mechanical changes. Lu et al. (29) demonstrated that treatment with the MMP inhibitor failed to prevent acute myocardial dysfunction and regional expansion after I/R injury. The duration of reperfusion in our study (180 min) and that in Lu et al. (90 min) (29) may be too short to detect a significant influence of MMP and TIMP on regional LV function, which may become evident after a longer period of reperfusion.

Table 3. *Hemodynamic parameters during cardiac microdialysis study*

	Baseline	150 min
HR, beat/min		
VNS	286±7	227±7*†
ACh	303±16	308±9
ACh-Atr	304±14	298±16
MAP, mmHg		
VNS	101±8	103±8
ACh	93±3	100±4
ACh-Atr	87±3	92±6
LV dP/dt_{max}, mmHg/s		
VNS	5,050±588	4,768±475
ACh	5,203±345	5,488±400
ACh-Atr	4,519±269	4,718±450
FS, %		
VNS	7.4±1.8	7.2±1.9
ACh	5.0±1.2	4.9±1.2
ACh-Atr	5.4±0.5	5.0±0.5

Values are means ± SE. VNS group, LV tissue was perfused with Ringer solution via a dialysis probe under vagal nerve stimulation; ACh group, LV tissue was perfused with Ringer solution containing ACh (1 mM) via a dialysis probe; ACh-Atr group, LV tissue was perfused with ACh (1 mM) and atropine (0.2 mM) via a dialysis probe. *$P < 0.01$ vs. ACh; †$P < 0.01$ vs. ACh-Atr.

Several previous studies (10, 35, 39) demonstrated that targeted deletion of MMP-9 and/or the upregulation of TIMP-1 reduced infarct size, prevented LV rupture, and ameliorated LV remodeling after MI. Conversely, the expression of other MMPs, such as MMP-2, has been shown to be important in the myocardial healing that occurs in the later phases after ischemic injury (10). These observations suggest that the beneficial effect of VNS on LV remodeling after MI observed in our previous study (23) may be in a part mediated through the modified expression of MMPs and TIMPs as noted in the present study.

Except for the post-MI LV remodeling, MMPs and TIMPs contribute to the progression of various cardiovascular disorders, including expansion and rupture of aortic aneurysm (44), progression of acute viral myocarditis (15), and restenosis after coronary intervention (12). Local overexpression of TIMP-1 prevented the expansion and rupture of aortic aneurysm in rats (3) or prevented cardiac injury and dysfunction during experimental viral myocarditis in mice (15). VNS may be an effective biological inducer of TIMP-1 for the treatment of these disorders.

Limitation

The present study examined a limited number of MMP and TIMP species over a very short duration after myocardial I/R. A number of MMP and TIMP species are expressed in the myocardium, and several have been identified to be upregulated in cardiac disorders (24). Myocardial MMP-1 (collagenase) is induced by I/R (29). The actions of MMP-1 are inhibited in part by TIMP-1 (31). These suggest that VNS may inhibit the activity of MMP-1 in myocardial I/R injury. Further studies to define the effect of VNS on the profile of MMPs and TIMPs expressed in the myocardium are warranted.

In the present study, VNS was started 15 min before coronary occlusion. We did not examine whether VNS started after the coronary artery occlusion or whether reperfusion is capable of increasing myocardial TIMP-1. The pretreatment strategy as adopted in this study is unrealistic in clinical practice. Therefore, further studies are required to examine the time factor of VNS.

Concentration of ACh perfused through the dialysis probe in this study (1 mM) was substantially higher than the dialysate concentration of endogenous ACh released from the myocardium (<20 nM) (1). The ACh concentration within the myocardial interstitium might have been elevated over the supraphysiological range in the present microdialysis study. However, even if the interstitial concentration of ACh was unphysiologically high, Atr blocked the increase in TIMP-1 expression in response to ACh stimulation. Therefore, it is fair to say that TIMP-1 expression in response to ACh stimulation is mediated through the muscarinic ACh receptor.

TIMP-1 binds with MMPs to form a rather high molecular weight complex. Our preliminary in vitro experiment demonstrated that the relative recovery of TIMP-1/lipocalin/MMP-9 complex (Calbiochem, La Jolla, CA) was 3.8 ± 1.3% (range 0–5.5%) and was lower than that for free TIMP-1 (11.1 ± 0.3%) (see METHODS). Although the presence of MMPs, especially MMP-9, could affect the measurement of TIMP-1 within the myocardium by our microdialysis method, this probably does not affect the conclusion drawn from the cardiac microdialysis study, because the study was conducted in a heart free of I/R, which might contain low levels of myocardial MMP-9 as inferred from the results of the I/R study.

CONCLUSION

In a rabbit model of myocardial I/R injury, VNS induced TIMP-1 expression in cardiomyocytes and reduced active MMP-9.

GRANTS

This study was supported by a grant-in-aid for Scientific Research (C) (18500358) from the Ministry of Education, Culture, Sports, Science and Technology; by Health and Labour Sciences research grants for research on medical devices for analyzing, supporting and substituting the function of human body (H15-physi-001) from the Ministry of Health, Labour and Welfare of Japan; and by a research grant from the Fukuda Foundation for Medical Technology.

REFERENCES

1. **Akiyama T, Yamazaki T.** Adrenergic inhibition of endogenous acetylcholine release on postganglionic cardiac vagal nerve terminals. *Cardiovasc Res* 46: 531–538, 2000.
2. **Akool el-S, Doller A, Muller R, Gutwein P, Xin C, Huwiler A, Pfeilschifter J, Eberhardt W.** Nitric oxide induces TIMP-1 expression by activating the transforming growth factor beta-Smad signaling pathway. *J Biol Chem* 280: 39403–39416, 2005.
3. **Allaire E, Forough R, Clowes M, Starcher B, Clowes AW.** Local overexpression of TIMP-1 prevents aortic aneurysm degeneration and rupture in a rat model. *J Clin Invest* 102: 1413–1420, 1998.
4. **Chandrasekar B, Smith JB, Freeman GL.** Ischemia-reperfusion of rat myocardium activates nuclear factor-KappaB and induces neutrophil infiltration via lipopolysaccharide-induced CXC chemokine. *Circulation* 103: 2296–2302, 2001.
5. **Cheung PY, Sawicki G, Wozniak M, Wang W, Radomski MW, Schulz R.** Matrix metalloproteinase-2 contributes to ischemia-reperfusion injury in the heart. *Circulation* 101: 1833–1839, 2000.
6. **Chua CC, Hamdy RC, Chua BH.** Angiotensin II induces TIMP-1 production in rat heart endothelial cells. *Biochim Biophys Acta* 1311: 175–180, 1996.
7. **Chua PK, Melish ME, Yu Q, Yanagihara R, Yamamoto KS, Nerurkar VR.** Elevated levels of matrix metalloproteinase 9 and tissue inhibitor of metalloproteinase 1 during the acute phase of Kawasaki disease. *Clin Diagn Lab Immunol* 10: 308–314, 2003.
8. **Crozier SJ, Vary TC, Kimball SR, Jefferson LS.** Cellular energy status modulates translational control mechanisms in ischemic-reperfused rat hearts. *Am J Physiol Heart Circ Physiol* 289: H1242–H1250, 2005.
9. **Dedkova EN, Ji X, Wang YG, Blatter LA, Lipsius SL.** Signaling mechanisms that mediate nitric oxide production induced by acetylcholine exposure and withdrawal in cat atrial myocytes. *Circ Res* 93: 1233–1240, 2003.
10. **Ducharme A, Frantz S, Aikawa M, Rabkin E, Lindsey M, Rohde LE, Schoen FJ, Kelly RA, Werb Z, Libby P, Lee RT.** Targeted deletion of matrix metalloproteinase-9 attenuates left ventricular enlargement and collagen accumulation after experimental myocardial infarction. *J Clin Invest* 106: 55–62, 2000.
11. **Ergul A, Walker CA, Goldberg A, Baicu SC, Hendrick JW, King MK, Spinale FG.** ET-1 in the myocardial interstitium: relation to myocyte ECE activity and expression. *Am J Physiol Heart Circ Physiol* 278: H2050–H2056, 2000.
12. **Feldman LJ, Mazighi M, Scheuble A, Deux JF, De Benedetti E, Badier-Commander C, Brambilla E, Henin D, Steg PG, Jacob MP.** Differential expression of matrix metalloproteinases after stent implantation and balloon angioplasty in the hypercholesterolemic rabbit. *Circulation* 103: 3117–3122, 2001.
13. **Fujimoto N, Zhang J, Iwata K, Shinya T, Okada Y, Hayakawa T.** A one-step sandwich enzyme immunoassay for tissue inhibitor of metalloproteinases-2 using monoclonal antibodies. *Clin Chim Acta* 220: 31–45, 1993.
14. **Gomez DE, Alonso DF, Yoshiji H, Thorgeirsson UP.** Tissue inhibitors of metalloproteinases: structure, regulation and biological functions. *Eur J Cell Biol* 74: 111–122, 1997.

15. **Heymans S, Pauschinger M, De Palma A, Kallwellis-Opara A, Rutschow S, Swinnen M, Vanhoutte D, Gao F, Torpai R, Baker AH, Padalko E, Neyts J, Schultheiss HP, Van de Werf F, Carmeliet P, Pinto YM.** Inhibition of urokinase-type plasminogen activator or matrix metalloproteinases prevents cardiac injury and dysfunction during viral myocarditis. *Circulation* 114: 565–573, 2006.
16. **Hudson MP, Armstrong PW, Ruzyllo W, Brum J, Cusmano L, Krzeski P, Lyon R, Quinones M, Theroux P, Sydlowski D, Kim HE, Garcia MJ, Jaber WA, Weaver WD.** Effects of selective matrix metalloproteinase inhibitor (PG-116800) to prevent ventricular remodeling after myocardial infarction: results of the PREMIER (Prevention of Myocardial Infarction Early Remodeling) trial. *J Am Coll Cardiol* 48: 15–20, 2006.
17. **Kameda K, Matsunaga T, Abe N, Hanada H, Ishizaka H, Ono H, Saitoh M, Fukui K, Fukuda I, Osanai T, Okumura K.** Correlation of oxidative stress with activity of matrix metalloproteinase in patients with coronary artery disease. Possible role for left ventricular remodelling. *Eur Heart J* 24: 2180–2185, 2003.
18. **Kao R, Rannels DE, Morgan HE.** Effects of anoxia and ischemia on protein synthesis in perfused rat hearts. *Circ Res* 38, *Suppl* 1: I124–I130, 1976.
19. **Kitagawa H, Yamazaki T, Akiyama T, Sugimachi M, Sunagawa K, Mori H.** Microdialysis separately monitors myocardial interstitial myoglobin during ischemia and reperfusion. *Am J Physiol Heart Circ Physiol* 289: H924–H930, 2005.
20. **Kodama S, Iwata K, Iwata H, Yamashita K, Hayakawa T.** Rapid one-step sandwich enzyme immunoassay for tissue inhibitor of metalloproteinases. An application for rheumatoid arthritis serum and plasma. *J Immunol Methods* 127: 103–108, 1990.
21. **La Rovere MT, Bigger JT Jr, Marcus FI, Mortara A, Schwartz PJ.** Baroreflex sensitivity and heart-rate variability in prediction of total cardiac mortality after myocardial infarction. ATRAMI (Autonomic Tone and Reflexes After Myocardial Infarction) Investigators. *Lancet* 351: 478–484, 1998.
22. **Le Quellec A, Dupin S, Genissel P, Saivin S, Marchand B, Houin G.** Microdialysis probes calibration: gradient and tissue dependent changes in no net flux and reverse dialysis methods. *J Pharmacol Toxicol Methods* 33: 11–16, 1995.
23. **Li M, Zheng C, Sato T, Kawada T, Sugimachi M, Sunagawa K.** Vagal nerve stimulation markedly improves long-term survival after chronic heart failure in rats. *Circulation* 109: 120–124, 2004.
24. **Li YY, Feldman AM, Sun Y, McTiernan CF.** Differential expression of tissue inhibitors of metalloproteinases in the failing human heart. *Circulation* 98: 1728–1734, 1998.
25. **Li YY, Feng Y, McTiernan CF, Pei W, Moravec CS, Wang P, Rosenblum W, Kormos RL, Feldman AM.** Downregulation of matrix metalloproteinases and reduction in collagen damage in the failing human heart after support with left ventricular assist devices. *Circulation* 104: 1147–1152, 2001.
26. **Lindsey M, Wedin K, Brown MD, Keller C, Evans AJ, Smolen J, Burns AR, Rossen RD, Michael L, Entman M.** Matrix-dependent mechanism of neutrophil-mediated release and activation of matrix metalloproteinase 9 in myocardial ischemia/reperfusion. *Circulation* 103: 2181–2187, 2001.
27. **Lindsey ML, Gannon J, Aikawa M, Schoen FJ, Rabkin E, Lopresti-Morrow L, Crawford J, Black S, Libby P, Mitchell PG, Lee RT.** Selective matrix metalloproteinase inhibition reduces left ventricular remodeling but does not inhibit angiogenesis after myocardial infarction. *Circulation* 105: 753–758, 2002.
28. **Livak KJ, Schmittgen TD.** Analysis of relative expression data using real-time quantitative PCR and the $2^{-\Delta\Delta C_t}$ method. *Methods* 25: 402–408, 2001.
29. **Lu L, Gunja-Smith Z, Woessner JF, Ursell PC, Nissen T, Galardy RE, Xu Y, Zhu P, Schwartz GG.** Matrix metalloproteinases and collagen ultrastructure in moderate myocardial ischemia and reperfusion in vivo. *Am J Physiol Heart Circ Physiol* 279: H601–H609, 2000.
30. **Mioni C, Bazzani C, Giuliani D, Altavilla D, Leone S, Ferrari A, Minutoli L, Bitto A, Marini H, Zaffe D, Botticelli AR, Iannone A, Tomasi A, Bigiani A, Bertolini A, Squadrito F, Guarini S.** Activation of an efferent cholinergic pathway produces strong protection against myocardial ischemia/reperfusion injury in rats. *Crit Care Med* 33: 2621–2628, 2005.
31. **Moe SM, Singh GK, Bailey AM.** Beta2-microglobulin induces MMP-1 but not TIMP-1 expression in human synovial fibroblasts. *Kidney Int* 57: 2023–2034, 2000.
32. **Mukherjee R, Brinsa TA, Dowdy KB, Scott AA, Baskin JM, Deschamps AM, Lowry AS, Escobar GP, Lucas DG, Yarbrough WM, Zile MR, Spinale FG.** Myocardial infarct expansion and matrix metalloproteinase inhibition. *Circulation* 107: 618–625, 2003.
33. **Pfeffer MA, Braunwald E.** Ventricular remodeling after myocardial infarction. Experimental observations and clinical implications. *Circulation* 81: 1161–1172, 1990.
34. **Romanic AM, Burns-Kurtis CL, Gout B, Berrebi-Bertrand I, Ohlstein EH.** Matrix metalloproteinase expression in cardiac myocytes following myocardial infarction in the rabbit. *Life Sci* 68: 799–814, 2001.
35. **Romanic AM, Harrison SM, Bao W, Burns-Kurtis CL, Pickering S, Gu J, Grau E, Mao J, Sathe GM, Ohlstein EH, Yue TL.** Myocardial protection from ischemia/reperfusion injury by targeted deletion of matrix metalloproteinase-9. *Cardiovasc Res* 54: 549–558, 2002.
36. **Silvestry SC, Taylor DA, Lilly RE, Atkins BZ, Marathe US, Davis JW, Kraus W, Glower DD.** The in vivo quantification of myocardial performance in rabbits: a model for evaluation of cardiac gene therapy. *J Mol Cell Cardiol* 28: 815–823, 1996.
37. **Squire IB, Evans J, Ng LL, Loftus IM, Thompson MM.** Plasma MMP-9 and MMP-2 following acute myocardial infarction in man: correlation with echocardiographic and neurohumoral parameters of left ventricular dysfunction. *J Card Fail* 10: 328–333, 2004.
38. **Stapel H, Kim SC, Osterkamp S, Knuefermann P, Hoeft A, Meyer R, Grohe C, Baumgarten G.** Toll-like receptor 4 modulates myocardial ischaemia-reperfusion injury: role of matrix metalloproteinases. *Eur J Heart Fail* 8: 665–672, 2006.
39. **Trescher K, Bernecker O, Fellner B, Gyongyosi M, Schafer R, Aharinejad S, DeMartin R, Wolner E, Podesser BK.** Inflammation and postinfarct remodeling: overexpression of IkappaB prevents ventricular dilation via increasing TIMP levels. *Cardiovasc Res* 69: 746–754, 2006.
40. **Udelson JE, Konstam MA.** Relation between left ventricular remodeling and clinical outcomes in heart failure patients with left ventricular systolic dysfunction. *J Card Fail* 8: S465–S471, 2002.
41. **Uemura S, Matsushita H, Li W, Glassford AJ, Asagami T, Lee KH, Harrison DG, Tsao PS.** Diabetes mellitus enhances vascular matrix metalloproteinase activity: role of oxidative stress. *Circ Res* 88: 1291–1298, 2001.
42. **Verheijen JH, Nieuwenbroek NM, Beekman B, Hanemaaijer R, Verspaget HW, Ronday HK, Bakker AH.** Modified proenzymes as artificial substrates for proteolytic enzymes: colorimetric assay of bacterial collagenase and matrix metalloproteinase activity using modified prourokinase. *Biochem J* 323: 603–609, 1997.
43. **Webb CS, Bonnema DD, Ahmed SH, Leonardi AH, McClure CD, Clark LL, Stroud RE, Corn WC, Finklea L, Zile MR, Spinale FG.** Specific temporal profile of matrix metalloproteinase release occurs in patients after myocardial infarction: relation to left ventricular remodeling. *Circulation* 114: 1020–1027, 2006.
44. **Wilson WR, Anderton M, Schwalbe EC, Jones JL, Furness PN, Bell PR, Thompson MM.** Matrix metalloproteinase-8 and -9 are increased at the site of abdominal aortic aneurysm rupture. *Circulation* 113: 438–445, 2006.
45. **Winer J, Jung CK, Shackel I, Williams PM.** Development and validation of real-time quantitative reverse transcriptase-polymerase chain reaction for monitoring gene expression in cardiac myocytes in vitro. *Anal Biochem* 270: 41–49, 1999.